Coil−Globule Transition of Poly(methyl methacrylate) in Acetonitrile

Yasuyuki Maki,* Naoki Sasaki, and Mitsuo Nakata

Department of Polymer Science, Faculty of Science, Hokkaido University, Sapporo 060-0810, Japan

Received April 23, 2004

ABSTRACT: The coil−globule transition was studied for poly(methyl methacrylate) (PMMA) in acetonitrile with molecular weights $M_w = 6.4 \times 10^6$ and 11.4×10^6 by static light scattering. Because of the very slow phase separation, the mean-square radius of gyration was determined reliably in the temperature range from above the Θ temperature at 44.0 °C down to 5 °C. PMMA chains in acetonitrile collapsed slowly to equilibrium globules, and the collapse processes were measured for time periods of 30 min to 7 days depending the molecular weight and temperature. The behavior of the equilibrium expansion factor was represented as a function of $(1 - \Theta/T)M^{1/2}$ and compared with the theoretical predictions by Birshtein and Pryamitsyn and those by Grosberg and Kuznetsov. The second and third virial coefficients for segment interactions were estimated from the observed coil−globule transition curve by using the theories and were comparable with literature values due to the second and third virial coefficients of the dilute solution.

1. Introduction

Ptitsyn first predicted the coil−globule transition of a polymer chain by introducing the third virial coefficient for segment interactions in the Flory theory of the expansion factor.[1] Since the theory showed that the chain collapse to a globule of small size would occur continuously or discontinuously depending on the magnitude of the third virial coefficient, the coil−globule transition has attracted much attention as a phenomenon analogous to the gas−liquid phase transition and to the conformational transition of biopolymers.[2−9] For usual polymer solutions, the chain collapse and the phase separation occur rapidly in the same temperature region and, consequently, the chain aggregation obscures observations of the coil−globule transition. However, the phase separation was found to occur very slowly for the solutions of poly(methyl methacrylate) (PMMA) in isoamyl acetate (IAA),[10−12] in *tert*-butyl alcohol (TBA),[13] and in the mixed solvent TBA + water (2.5 vol %),[14,15] and the expansion factor $\alpha^2 = \langle s^2\rangle/\langle s^2\rangle_o$ was determined reliably by static light scattering before the measurement was disturbed by chain aggregation, where $\langle s^2\rangle_o$ and $\langle s^2\rangle$ are the mean-square radii of gyration at and below the Θ temperature. The coil−globule transition curves obtained for PMMA in TBA and in the mixed solvent TBA + water (2.5 vol %) were close to each other and much steeper than that of PMMA in IAA. These experimental results were compared with the theoretical predictions by Grosberg and Kuznetsov,[7] and by Birshtein and Pryamitsyn.[6] The former authors calculated the expansion factor α^2 in a globule state based on the Lifshitz model[3] with the spatial density distribution into account. The latter authors derived an equation of the expansion factor based on the Flory model[9,16] in the form

$$\alpha^3 - \alpha - C(\alpha^{-3} - 1) = B\tau M^{1/2} \qquad (1)$$

by using the conformational entropy of a contracted polymer chain below the Θ temperature. Here, τ is the reduced temperature defined by $1 - \Theta/T$, M is the molecular weight, and B and C are related to the second and third virial coefficients among polymer segments, respectively. The above two theoretical predictions yield similar behavior of α^2 in a globule region.

Since the coefficients B and C in eq 1 can be easily determined from observed transition curves, eq 1 is useful for a phenomenological analysis of transition curves and gives an asymptotic behavior at large $|\tau M^{1/2}|$ as $\alpha^3 \sim -(C/B)/\tau M^{1/2}$. The values of the ratio C/B are roughly 3 for PMMA in TBA and in the mixed solvent and 17 in IAA, indicating that polymer chains in the former solvents collapse more densely than those in the latter solvent. The comparison between the observed transition curves and the theories supports the functional form of $\alpha^2 = \alpha^2(\tau M^{1/2})$ such as eq 1 but cannot verify the theories at a molecular level. For a stringent examination of the theories, the virial coefficients among segments should be estimated from transition curves and be compared with those obtained by a different kind of experiments.

In the present study, we carried out static light-scattering experiments on solutions of PMMA in acetonitrile for the molecular weight $M_w \times 10^{-6} = 6.4$ and 11.4 in the concentration range from 0.6×10^{-4} to 5×10^{-4} g/cm^3. For the solution, the second A_2 and the third virial coefficient A_3 among polymer chains have been measured, and the binary and ternary cluster integrals among polymer segments have been estimated.[17,18] Furthermore, the solution was found to undergo very slow phase separation, which permitted accurate light-scattering measurements even far below the Θ temperature. Thus, the virial coefficients among segments were deduced from the observed coil−globule transition curve and were compared with those due to the data of A_2 and A_3. A similar comparison for the virial coefficients was also made for a solution of polystyrene (PS) in cyclohexane with literature data.[19,20] For the solution,[21,22] the coil−globule transition was measured by light scattering for a sample with $M_w = 2.6 \times 10^7$ and $M_w/M_n = 1.3$ in the concentration range from 3×10^{-6} to 3×10^{-8} g/cm^3. This large molecular weight and low concentration were employed on account of the rapid phase separation. To demonstrate the extremely different rates of phase

* To whom correspondence should be addressed.

10.1021/ma049208l CCC: $27.50
Published on Web 07/02/2004

separation between the two solutions of PMMA in acetonitrile and PS in cyclohexane, chain aggregation processes in the solutions were measured by light scattering.

2. Experiment

Samples and Solution Preparation. In a previous study,[11] PMMA was prepared by bulk polymerization of methyl methacrylate with 2,2′-azobis(isobutyronitrile) of 0.0025 wt % at 50.0 °C. The PMMA was fractionated into 11 fractions (series M21) by fractional solution method. In this study, two fractions designated by M21-AF5 and M21-F8 were used as samples. The sample M21-F8 is the eighth fraction of the series M21. The third and fourth fractions of M21 were combined and further fractionated into eight fractions (series A) by the solution method. M21-AF5 is the fifth fraction of series A. The weight-average molecular weight M_w was determined to be $M_w \times 10^{-6} = 6.4$ and 11.4 by light scattering, and the ratio of M_w to the number-average molecular weight M_n was determined to be $M_w/M_n = 1.25$ and 1.34 by analytical gel permeation chromatography for M21-AF5 and M21-F8, respectively. Acetonitrile was fractionally distilled immediately before use.

The solution for light-scattering measurement was prepared at four concentrations near c (10^{-4} g/cm^3) = 1.1, 2.2, 3.2, 4.5 for M21-AF5 and c (10^{-4} g/cm^3) = 0.7, 1.5, 2.3, 3.0 for M21-F8. Each solution was prepared by diluting a stock solution in an optical cell of 18 mm i.d. and 1 mm in wall thickness that is sealed tightly with a Teflon cap to prevent evaporation of the solvent. The optical cells were kept under saturated vapor of acetonitrile in the dark near the Θ temperature for a few days to sediment impurity particles to the bottom of cell, which made the optical clarification of the solution effectively.

Static Light Scattering. Each optical cell preserved near the Θ temperature was transferred into a thermostated cylindrical cell at the center of a photometer, and the measurement of scattered light was started 30 min after the setup of the cell to allow sufficient time for thermal equilibration. The measurement was carried out over the angular range 30−150° at intervals of 15° with vertically polarized incident light at 632.8 nm from a He−Ne laser. The photometer was calibrated with benzene, taking its Rayleigh ratio as 12.63×10^{-6} cm^{-1}.[23] The light-scattering data were obtained in the temperature ranges of 5 °C to 44 for M21-AF5 and of 10 °C to 60 for M21-F8.

The temperature t(°C) dependence of the refractive index increment dn/dc (cm^3/g) at 632.8 nm was obtained as dn/dc = $0.1284 + (3.3 \times 10^{-4})t$ in the temperature range 20−45 °C by using a differential refractometer of the Brice-type. This relation was used beyond the temperature range in the data analysis.

To determine the molecular weight M_w, the z-average mean-square radius of gyration $\langle s^2\rangle_z$ and the second virial coefficients A_2 with the light-scattering data, the excess Rayleigh ratio R_θ at an angle θ was analyzed by the scattering equation[24]

$$(Kc/R_\theta)^{1/a} = (1/M_w^{1/a})\{1+(1/3a)\langle s^2\rangle_z q^2 + (2/a)M_w A_2 c\} \quad (2)$$

with $K = (4\pi^2 n^2/N_A\lambda^4)(\mathrm{d}n/\mathrm{d}c)^2$ and $q = (4\pi n/\lambda)\sin(\theta/2)$, where N_A is Avogadro's number, λ is the wavelength of incident light in a vacuum, and n is the refractive index of solution. The plot of $(Kc/R_\theta)^{1/a}$ vs $\sin^2(\theta/2)$ should give a straight line for an appropriate value of the constant a, and $\langle s^2\rangle_z$ can be determined from the slope of the plot.[24]

Light-scattering data were analyzed by the Zimm plot due to eq 2 with $a = 1.5$, and the characteristic ratio at the Θ temperature was estimated to be $\langle s^2\rangle_{oz}/M_w = 6.3 \times 10^{-18}$ cm^2 for M21-AF5 and 6.9×10^{-18} cm^2 for M21-F8.

3. Experimental Results

Analyses of Light Scattering Data. Figure 1 shows light-scattering data of the sample M21-F8 ($M_w = 1.14 \times 10^7$) in a form of the Zimm plot due to eq 2. The plots a (circle) and b (square) were obtained at 60 min and at 11 580 min after quenching to 10 °C, respectively. In each plot, the data points for a dependence on $\sin^2(\theta/2)$ are described by the straight lines with a same slope and extrapolated to $\theta = 0$ as indicated by the filled symbols. The slope was used to estimate $\langle s^2\rangle_z$. The decrease of the slope with the time suggests a slow chain collapse. In plot a, the filled points at $\theta = 0$ are described by the straight line, while in plot b, the filled points at two lower concentrations are used for the straight line on account of a chain aggregation effect due to the phase separation at high concentrations. The straight line fitted to the two points yields the same intercept as that of the plot a at 60 min. Thus, the parallel lines for the $\sin^2(\theta/2)$ dependence and the common intercept at $\theta = 0$ and $c = 0$ demonstrate that the determination of M_w and $\langle s^2\rangle_z$ is not disturbed by an effect of phase separation. Data of the second virial coefficient A_2 were discarded because the effect of chain aggregation on A_2 cannot be shown clearly. The common intercept of the plots in Figure 1 yields somewhat higher value for the molecular weight. This is mainly attributed to a difficulty in measuring the incident intensity of the thin laser beam after passing through an optical cell. A slight deflection of the incident light by the cell sometimes yielded an underestimation of the incident intensity and resulted in a higher molecular weight. However, this uncertainty does not affect the estimation of $\langle s^2\rangle$ according to eq 2. Moreover, to discuss the coil−globule transition, we use the expansion factor $\alpha^2 = \langle s^2\rangle/\langle s^2\rangle_o$ for which the effect of the molecular weight distribution could be minimized.

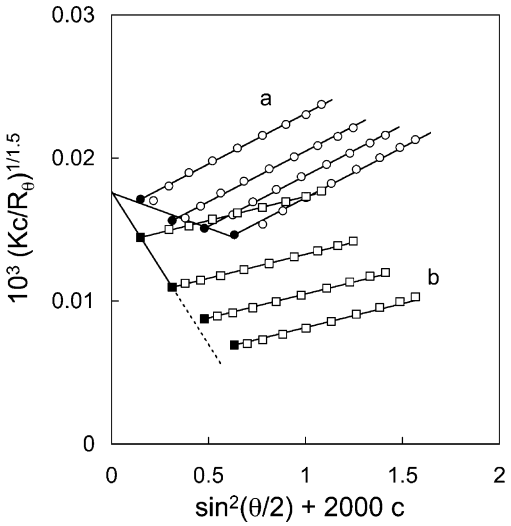

Figure 1. Zimm plot of $(Kc/R_\theta)^{1/1.5}$ as a function of $\sin^2(\theta/2)$ and c (g/cm^3) for light-scattering data of PMMA with $M_w = 1.14 \times 10^7$ in acetonitrile. Plots a (circles) and b (squares) were obtained at 60 and 11 580 min after quenching to 10 °C, respectively.

Chain Collapse Processes. Figures 2 and 3 illustrate chain collapse processes at various temperatures for $M_w = 6.4 \times 10^6$ and 1.14×10^7, respectively. The process is shown by plotting the transient expansion factor $\alpha^2(t)$ against ln t, where t is the time in minutes. The plots from the top to the bottom in Figures 2 and 3 were obtained at 25.0, 20.0, 15.0, 10.0, and 5.0 °C and at 30.0, 20.0, and 10.0 °C, respectively. The chain collapse process depends strongly on the molecular weight and temperature. At higher temperatures than those indicated above, the chain contraction was so fast that the equilibrium chain size was reached within about 60 min after the quench. This situation is inferred

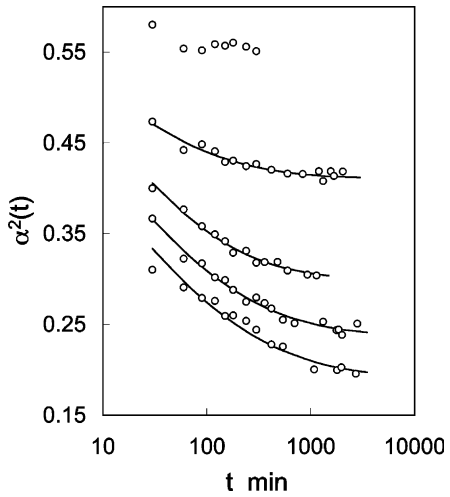

Figure 2. Chain collapse processes for $M_w = 6.4 \times 10^6$ by the plot of α^2 vs ln t with the time t in minute. The plots from the top to the bottom were obtained at 25.0, 20.0, 15.0, 10.0, and 5.0 °C. The lines are given by eq 3 with appropriate values of α_∞^2, τ_c, and β.

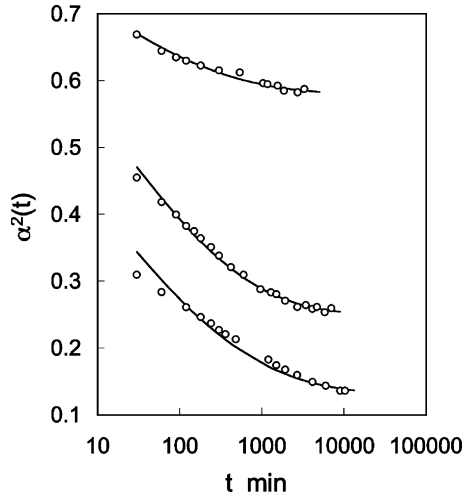

Figure 3. Chain collapse processes for $M_w = 1.14 \times 10^7$ by the plot of α^2 vs ln t with the time t in minute. The plots from the top to the bottom were obtained at 30.0, 20.0, and 10.0 °C. The lines are given by eq 3 with appropriate values of α_∞^2, τ_c, and β.

from the plot at 25.0 °C in Figure 2. At lower temperatures, equilibrium expansion factors would be estimated by extrapolating the behavior of data points to sufficiently large t.

In the previous studies for PMMA in IAA and in the mixed solvent of TBA + water (2.5 vol %), the chain contraction process was expressed by the stretched exponential function[14]

$$\alpha^2(t) = \alpha_\infty^2 + (1 - \alpha_\infty^2) \exp[-(t/\tau_c)^\beta] \qquad (3)$$

where β and τ_c are constant independent of the time t, and α_∞^2 is an equilibrium expansion factor. The plot of $\ln[(1 - \alpha_\infty^2)/(\alpha^2 - \alpha_\infty^2)]$ vs ln t for each collapse process was linear when an appropriate value was assigned to α_∞^2, and consequently, values of β and τ_c were estimated from the slope and intercept of the linear plot. For the present data, the plot also yielded straight lines when an appropriate value of α_∞^2 was chosen. The value of α_∞^2 was slightly smaller than those obtained in the last time range of measurement. The difference was no more than 5%. The values of β and τ_c obtained from the straight lines scattered between 0.21 and 0.26 and between 0.8 min and 13.5, respectively. These values were comparable with those obtained in the previous study.[14] The solid lines in Figures 2 and 3 are depicted by eq 3 with the values α_∞^2, β, and τ_c.

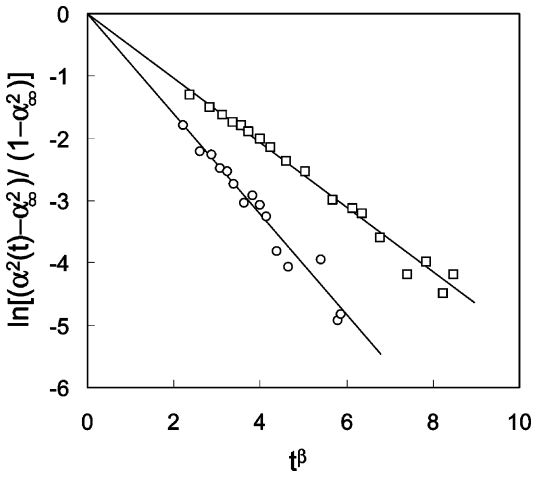

Figure 4. Chain collapse process at 10.0 °C for $M_w = 6.4 \times 10^6$ (circles) and at 20.0 °C for $M_w = 1.14 \times 10^7$ (squares) by the plot according to eq 3 with appropriate values of α_∞^2 and β.

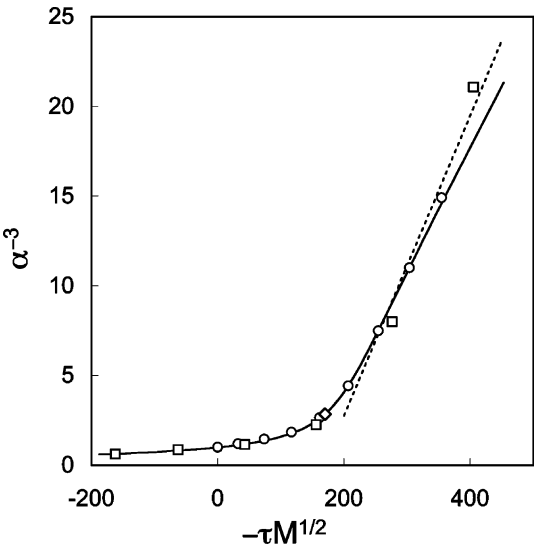

Figure 5. Coil−globule transition curve by the plot of α^{-3} vs $\tau M^{1/2}$ for PMMA in acetonitrile with $M_w = 6.4 \times 10^6$ (circles) and $M_w = 1.14 \times 10^7$ (squares). The solid curve is given by eq 1 with $B = 0.0025$ and $C = 0.041$. The diamond represents a crossover point between coil and globule regions. The broken straight line is fitted to data points in the globule region.

Figure 4 shows the plot of $\ln[(\alpha^2 - \alpha_\infty^2)/(1 - \alpha_\infty^2)]$ vs t^β at 10 °C for $M_w = 6.4 \times 10^6$ (circles) and at 20.0 °C for $M_w = 11.4 \times 10^6$ (squares). The plot gives the straight lines passing the origin, which confirms the validity of eq 3 for the present data. The two chain collapse processes have nearly the same values of $\alpha_\infty^2 \sim 0.25$ but are obviously different in the rate of chain collapse because of the different molecular weights.

Equilibrium Expansion Factor. Figure 5 exhibits the behavior of the equilibrium expansion factor α^2 by a plot of α^{-3} vs $-\tau M^{1/2}$. The circle and square show the data for $M_w \times 10^{-6} = 6.4$ and 11.4, respectively. At higher temperatures, the equilibrium expansion factor was directly determined within 60 min after quench,

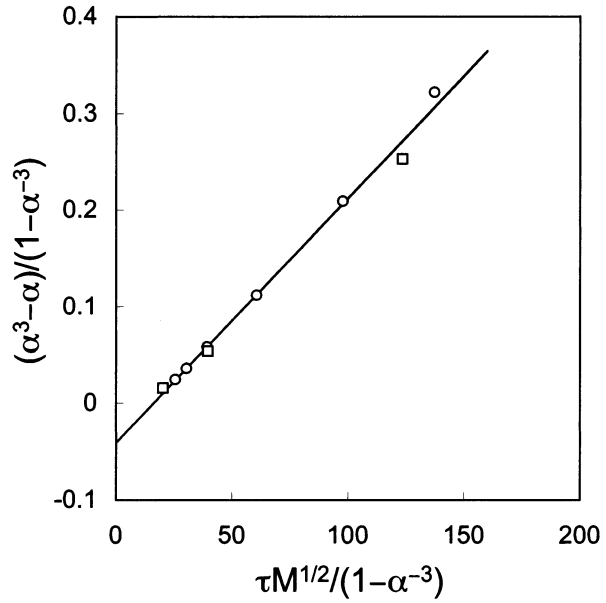

Figure 6. Plot according to eq 1 for PMMA in acetonitrile. The open circles and squares are for $M_w = 6.4 \times 10^6$ and $M_w = 1.14 \times 10^7$, respectively. The straight line gives the coefficients in eq 1 as $B = 0.0025$ and $C = 0.041$.

while at low temperatures the expansion factor was obtained as α_∞^2 with eq 3. The data points construct a single curve. This means that the analysis by eq 3 gives a reasonable estimation of the equilibrium expansion factor, because the uncertainty of the small value of α^2 is exaggerated in the reciprocal behavior of α^{-3}.

According to eq 1, the plot of $(\alpha^3 - \alpha)/(1 - \alpha^{-3})$ vs $\tau M^{1/2}/(1 - \alpha^{-3})$ for $\alpha < 1$ should give a straight line, whose slope and intercept could be used to estimate B and C, respectively. Figure 6 shows the plot with the same symbols as those in Figure 5. Data points near the Θ temperature are omitted because of large scattering due to the value of α close to unity. From the straight line fitted to the data points, we obtained $B = 0.0025$ and $C = 0.041$. The solid line in Figure 5 is described by eq 1 with the values of B and C. The crossover point between coil and globule states has been assumed to be located at the inflection point on the curve of α^2 vs $\tau M^{1/2}$ and, accordingly, can be calculated as $\alpha^2 = 0.468$ and $\tau M^{1/2} = -168$ with the aid of eq 1.[10] The diamond on the solid line in Figure 5 shows the crossover point.

4. Discussion and Conclusion

Comparison with the Theory by Grosberg and Kuznetsov. They analyzed the chain behavior in a globule state based on the Lifshitz model[3] and derived the expansion factor in the form[7]

$$\alpha = P^{1/2}\alpha^*(x) \tag{4}$$

$$x = Q\tau M^{1/2} \tag{5}$$

where $\alpha^*(x)$ is a reduced function, and the parameters P and Q are defined respectively by

$$P = w^{1/2}/a^3 \tag{6}$$

$$Q = (6^{3/2} N/M)^{1/2} (v/w^{1/2})(w^{1/2}/a^3)^{1/2} \tag{7}$$

Here, a is the size of a segment, N is the number of segments in a chain, and $\tau v = (1 - \Theta/T)v$ and w represent the second and third virial coefficients in the expansion of the free energy of segment interactions, respectively. The reduced function $\alpha^*(x)$ has been calculated numerically in the globule region of $-10.0 > x > -501.0$. The crossover point between coil and globule was assumed to be given by $x = -10.2$, at which the globule free energy vanishes. In the range $-11.1 > x > -174$ of the usual experiment, the numerical result can be approximated within an error of 3% by

$$\alpha^{*-3}(x) = g + hx \tag{8}$$

with $g = -0.70$ and $= -0.084$. The asymptotic relation of eq 8 at large $-x$ is close to $\alpha^{*-3} \sim -0.0800x$ due to the volume approximation at $x \to -\infty$.[7] From eqs 4 and 8, we obtain

$$P^{3/2}\alpha^{-3} = g + hQ\tau M^{1/2} \tag{9}$$

Thus, the plot of α^{-3} vs $\tau M^{1/2}$ should yield a straight line of which the intercept and slope can be used to estimate P and Q. The virial coefficients v and w can be estimated from P and Q by using eqs 6 and 7, because the segment size a and N can be estimated from the observed characteristic ratio $\langle s^2\rangle_o/M = a^2N/6$ and the molecular weight $m = M/N$ of a monomer. We used $\langle s^2\rangle_o/M = 5.4 \times 10^{-18}$ cm^2 and $m = 100$ for the PMMA solution. The former value was obtained by correcting the observed characteristic ratio $\langle s^2\rangle_{oz}/M_w$ for the molecular weight distribution by $\langle s^2\rangle_{ow}/M_w = (\langle s^2\rangle_{oz}/M_w)(1 + U)/(1 + 2U)$, where U is given by $M_w/M_n = 1 + U$.[26] We obtained $\langle s^2\rangle_o/M \times 10^{18} = 5.3$ cm^2 and 5.5 for $M_w \times 10^{-6} = 6.4$ and 11.4, respectively, and employed the average value.

Data points in the globule region in Figure 5 may be fitted by the broken straight line, which gives values of the parameters P and Q, and, correspondingly, values of v and w as shown in the first row in Table 1. We also analyzed data of the coil−globule transition curve for PMMA in IAA,[10] in TBA,[13] and in the mixed solvent TBA + water (2.5 vol %)[14] and for PS in cyclohexane.[22] The obtained values of the parameters P, Q, v, and w are listed in Table 1. For polystyrene in cyclohexane, the data was read from the plot in Figure 2 in ref 22, and the parameters were obtained with $\langle s^2\rangle_o/M = 8.8 \times 10^{-18}$ cm^2 and $m = 104$[25] by omitting two data points at the largest $-\tau M^{1/2}$ (see Figure 11 in ref 14). The last row in Table 1 shows the result of the previous analysis with these points into account.

Comparison with the Birshtein and Pryamitsyn Theory. Table 2 gives the experimental values of the parameters B and C in eq 1. The present values for PMMA in acetonitrile are shown in the first row. We have also analyzed the data for other systems mentioned above and determined B and C as shown in Table 2. The values of B and C are substantially same as those determined in the previous studies except for in the case of PS in cyclohexane, for which the previous values are given in the last row. The different values of the parameters obtained by the two analyses may indicate a possible error in the data treatment. Equation 1 has a critical point at $B\tau M^{1/2} = -0.4135$ and $\alpha^2 = 0.4714$ for $C = 0.00549$: The transition curve due to eq 1 is continuous for $C > 0.00549$ and discontinuous for $C < 0.00549$. Figure 7 shows a comparison of the transition curves for PMMA in acetonitrile (curve a), in IAA (curve b) and in TBA (curve c) by plotting α^2 against $\tau M^{1/2}$. The

Table 1. Results of Analyses of Coil−Globule Transition Curves of Various Systems by Eq 9

solutions	P	Q	$v \times 10^{23}$ cm^3	$w \times 10^{45}$ cm^6	v_G/v_B	w_G/w_B
PMMA + acetonitrile	0.136	0.050	0.88	0.63	2.1	1.6
PMMA + IAA	0.32	0.118	3.2	3.4	4.8	5.4
PMMA + TBA	0.24	0.48	11	2.0	3.7	3.6
PMMA + mixed solvent	0.21	0.44	10	1.5	3.4	3.6
PS + cyclohexane	0.13	0.36	14	2.8	2.0	1.7
PS + cyclohexane[a]	0.16	0.45	19	4.1	3.2	3.4

[a] Previous study[14]

Table 2. Results of Analyses of Coil−Globule Transition Curves of Various Systems by Eq 1

solutions	B	C	C/B	$v \times 10^{23}$ cm^3	$w \times 10^{45}$ cm^6
PMMA + acetonitrile	0.0025	0.041	16.4	0.42	0.39
PMMA + IAA	0.0039	0.067	17.2	0.66	0.64
PMMA + TBA	0.0183	0.057	3.1	3.1	0.55
PMMA + mixed solvent	0.0167	0.043	2.6	2.8	0.41
PS + cyclohexane	0.0183	0.034	1.9	7.0	1.6
PS + cyclohexane[a]	0.0159	0.026	1.6	6.1	1.2

[a] Previous study.[14]

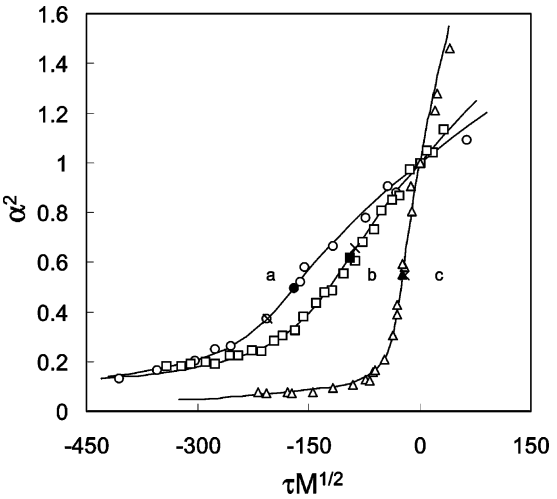

Figure 7. Coil−globule transition curves by the plot of α^2 vs $\tau M^{1/2}$ for PMMA in acetonitrile (circles), in IAA (squares) and in TBA (triangles). The filled symbols and crosses represent the coil−globule crossover points calculated as the inflection point and by the relation $Q\tau M^{1/2} = -10.2$, respectively.

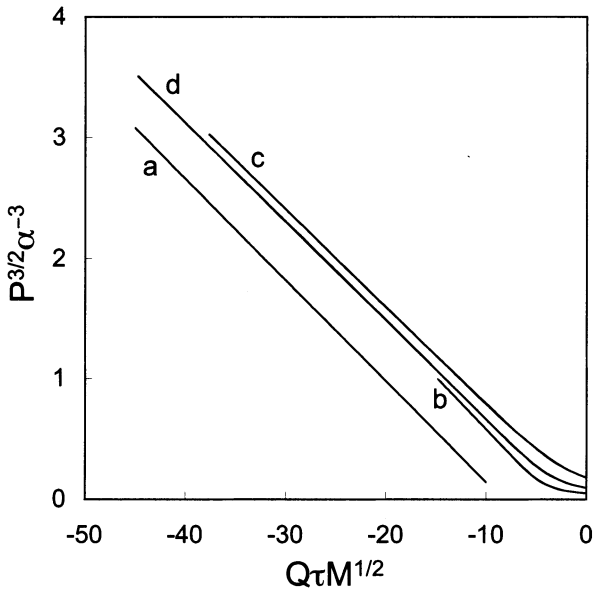

Figure 8. Comparison between eq 1 and eq 4 by the reduced plot. Equation 4 gives line a, and eq 1 gives curves b, c, and d, which are described with P and Q obtained for PMMA in acetonitrile, in IAA, and in the mixed solvent, respectively. The straight line portion of each plot corresponds to the range in which the experimental data were analyzed by eqs 1 and 4.

transition curve for PMMA in the mixed solvent is not distinguished from that in TBA in the plot. The coil−globule transition is sharp in TBA and broad in acetonitrile. The filled symbols on each curve indicate the coil−globule crossover point calculated as an inflection point with eq 1. On account of the small value of C, the transition curve in acetonitrile would be expected to be sharp. However, this is not the case. The small value of B in acetonitrile makes the transition broad. The transition curves for acetonitrile and IAA have the crossover point at different values of α^2 but show similar behavior at large $-\tau M^{1/2}$. The asymptotic behavior of eq 1 is given by $\alpha^3 \sim -(C/B)/\tau M^{1/2}$, and the ratio C/B is nearly the same for these solvents. The cross on each curve indicates the coil−globule crossover point due to the prediction $x \sim -10.2$.[7] The crossover points by the two estimations are not so different.

The parameters of B and C in eq 1 have been related explicitly to the second $v\tau$ and the third virial coefficient w of segment interactions, respectively. The relations are obtained by assigning the volume $V = \sigma\langle s^2\rangle^{3/2}$ occupied by a single chain. At a globule state, it is reasonable to use $(4\pi/3)(^5/_3)^{3/2}$ for the numerical constant σ on account of a uniform segment distribution in a sphere.[7] Thus, the parameters are written as

$$B = 1.09v(N/M)^{1/2}/a^3 \quad (10)$$

$$C = 3.55w/a^6 \quad (11)$$

Since the values of a and N have been obtained already, the values of v and w due to B and C are readily estimated as given in Table 2.

Experimental Examination of Theoretical Predictions. The virial coefficients due to eq 9 is considerably larger than those due to eq 1. In Table 1 the ratios of the virial coefficients by eq 9 to those by eq 1 are given as v_G/v_B and w_G/w_B, which are nearly the same for each solution and appear to change with P. Since the parameters B and C are related to P and Q as $B = 0.284QP^{1/2}$ and $C = 3.55P^2$, eq 1 can be compared directly with eq 9. Figure 8 exhibits the plot of $P^{3/2}\alpha^{-3}$ vs $x = Q\tau M^{1/2}$. The plot a is given by eq 9, and plots b, c, and d are described by eq 1 with the values of B and C for PMMA in acetonitrile, in isoamyl acetate, and in

Table 3. Comparison of the Second v and the Third Virial Coefficients w Obtained from Coil−Globule Transition Curve and from Virial Coefficients A_2 and A_3 of the Solution

	PMMA in acetonitrile		PS in cyclohexane	
	$v \times 10^{23}$ cm^3	$w \times 10^{45}$ cm^6	$v \times 10^{23}$ cm^3	$w \times 10^{45}$ cm^6
Birshtein and Pryamitsyn (eq 1)	0.42	0.39	7.0	1.6
Grosberg and Kuznetsov (eq 9)	0.88	0.63	14	2.8
A_2, A_3	1.75	0.8	4.5	0.7

the mixed solvent, respectively. The straight line portion of the plot corresponds to the region where the values of P and Q were estimated from experimental data. Plots b, c, and d are close to each other and can be represented by nearly straight lines except for in the range $x > -5$. The straight line portion of plots b, c, and d gives the values of $(-g, -h)$ in eq 9 as (0.306, 0.087), (0.028, 0.081) and (0.154, 0.082), respectively. The asymptotic relation of eq 1 at large $-x$ is given by $\alpha^{-3} \sim -(B/C)\tau M^{1/2} = -0.0800x/P^{3/2}$, which agrees with that of eq 4. Correspondingly, the values of h for plots b, c, and d are close to $h = -0.084$ in eq 8. Thus, the main difference between eqs 1 and 4 in the globule region is reflected to the value of g, and the reduced form of eq 1 is not represented uniquely by x. The variation of the ratios v_G/v_B and w_G/w_B may be in accord with the change of the estimated g.

The second $v\tau$ and third virial coefficient w in free energy expansion of segment interactions can be related to the binary β_2 ($=\beta_o\tau$) and the ternary cluster integral β_3 among segments by $v\tau = \beta_2/2$ and $w = \beta_3/6$, respectively. For the solutions of PMMA in acetonitrile and PS in cyclohexane, both β_2 and β_3 have been estimated from the experimental values of the virial coefficients A_2 and A_3 for the dilute solutions. For the PMMA solution,[17] the temperature dependence of β_2 above and below the Θ temperature was expressed by $\beta_2 = \beta_o\tau$ with $\beta_o = 3.5 \times 10^{-23}$ cm^3 while, for the PS solution,[19] β_2 below the Θ temperature was not linear to τ, but we roughly estimated $\beta_o = 9 \times 10^{-23}$ cm^3 in the limited range $0 > \tau > -0.04$ of the experiment by Tanaka et al. The ternary cluster integral has been determined to be $\beta_3 \times 10^{45} = 4.8$ and 4.4 for the PMMA and PS solutions, respectively.[18] The values of v and w due to β_o and β_3 are given in Table 3 and are compared with those from the coil−globule transition curves. The values of v and w from A_2 and A_3 are close to those by eq 9 for PMMA in acetonitrile and to those by eq 1 for PS in cyclohexane. Thus, the virial coefficients due to the coil−globule transition curves may be comparable with those due to A_2 and A_3. However, it is not conceivable that the coil−globule transition curves of the PMMA and PS solutions obey different laws such as eq 9 and eq 1, respectively. This contradiction may be attributed to experimental difficulty below the Θ temperature particularly for the solution of PS in cyclohexane. On account of the rapid chain aggregation of PS in cyclohexane, Tanaka et al. determined the phase separation temperature at extreme conditions of molecular weight and concentration as mentioned in Introduction and carried out light-scattering measurements above the cloud point curve. Thus, Tanaka et al. first demonstrated chain collapse by measuring the coil−globule transition curve. At present, however, the transition curve does not seem to be accurate enough for estimation of the virial coefficient v and w. They determined the Θ temperature as 35.4 °C, at which the characteristic ratio $\langle s^2\rangle_{oz}/M_w$ is read as 13.2×10^{-18} cm^2 from the plot in Figure 2 in ref 22. This value is very large compared with 8.8×10^{-18} cm^2 even after a correction for the molecular weight distribution $M_w/M_n = 1.3$.[25] Though we are not certain about the reason for the large value, considerable uncertainty should be assumed for the coil−globule transition curve. On the other hand, Chu et al. observed a chain collapse process of PS in cyclohexane with $M_w = 8.1 \times 10^6$ for about 10 min.[27] It is not certain whether Tanaka et al. observed equilibrium expansion factors for the large molecular weight $M_w = 2.6 \times 10^7$ or not. Thus, we cannot take the values of v and w from the transition curve of PS in cyclohexane seriously.

Experimental Difficulties due to Chain Aggregation. Since the study by Tanaka et al.,[21,22] the coil−globule transition curve has not been measured for PS solutions because of a rapid chain aggregation due to phase separation. To see the experimental difficulty we compared the chain aggregation process of PS in cyclohexane to that of PMMA in acetonitrile by light scattering. We prepared the nearly same solutions in concentration and in molecular weight as $c = 1.1 \times 10^{-4}$ g/cm^3 and $M_w = 7.1 \times 10^6$ for the PS solution and $c = 1.3 \times 10^{-4}$ g/cm^3 and $M_w = 6.4 \times 10^6$ for the PMMA solution. First, we tried to measure the chain aggregation process 15 K below the phase separation temperature, but the measurement could not follow the rapid chain aggregation in the PS solution. Then, we tried to measure the chain aggregation process 1 K below the phase separation temperature. However the chain aggregation in the PMMA solution was so slow that the increase of scattered intensity was hardly observed in a time scale of week. Thus, the chain aggregation process was measured 1 and 15 K below the phase separation temperature for polystyrene and PMMA solutions, respectively. As a measure of chain aggregation, (R_θ/Kc) at the angle $\theta = 30$ was used, because the plot of $(Kc/R_\theta)^{1/1.5}$ vs $\sin^2(\theta/2)$ was linear for the PMMA solution but curved strongly at lower angles for the polystyrene solution, which hindered the extrapolation to $\theta = 0$. Figure 9 exhibits the observed chain aggregation processes by the plot of $\ln(R_{30}/Kc)$ vs time t min. The squares and circles are for the chain aggregation processes for the PMMA and PS solutions, respectively. The circles on the ordinate indicate very fast chain aggregation. To make the process visible, the data of PS are plotted in an enlarged time scale in the inset. The increase of $\ln(R_{30}/Kc)$ to ∼19 requires 60 min for the PS solution and 15 000 min (10 days) for the PMMA solution. This difference will become much larger for experiments carried out at a same quench depth from the phase separation temperature. Thus, the rates of chain aggregation of the two solutions cannot be compared properly because of the too large difference. This explains that Tanaka et al. explored the chain collapse above the phase separation temperature by using a solution of very low concentrations and very high molecular weight.

Yamakawa scrutinized experimental data of α^2 for PS in cyclohexane below the Θ temperature but in the stable region.[19,28] Thus, the data were confined in the range $\alpha^2 > 0.5$ and fell between the first- and second-

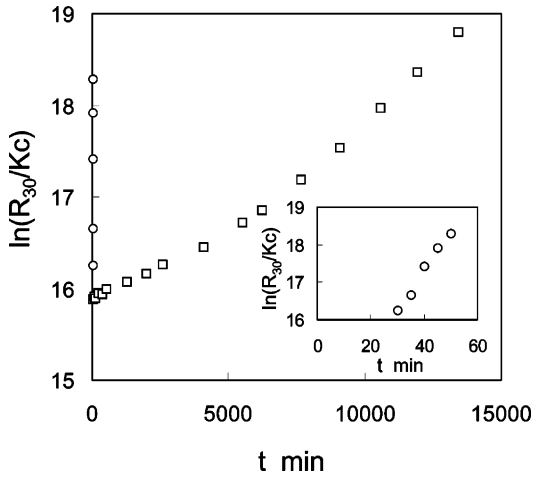

Figure 9. Comparison between chain aggregation processes of PMMA in acetonitrile (squares) and PS in cyclohexane (circles) by plotting $\ln(Kc/R_\theta)$ at the angle $\theta = 30$ against the time t. The scattered intensities were measured 1 and 15 K below the phase separation temperature for PS and PMMA solutions, respectively. Both the solutions were prepared near the concentration $c \sim 1.2 \times 10^{-4}$ g/cm^3 and with samples near $M_w \sim 7 \times 10^6$. The inset exhibits the chain aggregation process for PS in an enlarged time scale.

order perturbation calculations. Consequently, the analysis by Yamakawa showed that the experiments for the PS solutions, though carried out carefully, provided little information on the coil−globule transition. In marked contrast to the PS solution, PMMA solutions undergo extremely slow phase separation and the coil−globule transition can be measured below the phase separation temperature by light scattering.

Acknowledgment. This work was supported by a Grant-in-Aid for Scientific Research (B) (Grant No. 14340117) from the Ministry of Education, Science, Sport, and Culture of Japan.

References and Notes

(1) Ptitsyn, O. B.; Kron, A. K.; Eizner, Y. Y. *J. Polym. Sci., Part C* **1968**, *16*, 3509.
(2) de Gennes, P. G. *J. Phys. (Paris) Lett.* **1975**, *36*, L55-L57.
(3) Lifshitz, I. M.; Grosberg, A. Y.; Khokhlov, A. R. *Rev. Mod. Phys.* **1978**, *50*, 683.
(4) Post, C. B.; Zimm, B. H. *Biopolymers* **1979**, *18*, 1487.
(5) Sanchez, I. C. *Macromolecules* **1979**, *12*, 980.
(6) Birshtein, T. M.; Pryamitsyn, V. A. *Macromolecules* **1991**, *24*, 1554.
(7) Grosberg, A. Y.; Kuznetsov, D. V. *Macromolecules* **1992**, *25*, 1970; **1992**, *25*, 1980; **1992**, *25*, 1991.
(8) Grosberg, A. Y.; Khokhlov, A. R. *Statistical Physics of Macromolecules*; AIP Press: New York, 1994.
(9) Grosberg, A. Y.; Khokhlov, A. R. *Giant Molecules*; Academic Press: New York, 1997.
(10) Nakata, M.; Nakagawa, T. *Phys. Rev. E* **1997**, *56*, 3338.
(11) Nakata, M.; Nakagawa, T. *J. Chem. Phys.* **1999**, *110*, 2703.
(12) Nakata, M.; Nakagawa, T.; Nakamura, Y.; Wakatsuki, S. *J. Chem. Phys.* **1999**, *110*, 2711.
(13) Nakamura, Y.; Sasaki, N.; Nakata, M. *J. Chem. Phys.* **2003**, *118*, 3861.
(14) Nakamura, Y.; Sasaki, N.; Nakata, M. *Macromolecules* **2001**, *34*, 5992.
(15) Nakamura, Y.; Nakagawa, T.; Sasaki, N.; Yamagishi, A.; Nakata, M. *Macromolecules* **2001**, *34*, 5984.
(16) Flory, P. J. *Principles of Polymer Chemistry*; Cornell University Press: New York, 1953.
(17) Abe, F.; Einaga, Y.; Yamakawa, H. *Macromolecules* **1995**, *28*, 694.
(18) Yamakawa, H.; Abe, F.; Einaga, Y. *Macromolecules* **1994**, *27*, 3272.
(19) Yamakawa, H.; Abe, F.; Einaga, Y. *Macromolecules* **1994**, *27*, 5704.
(20) Nakamura, Y.; Norisuye, T.; Teramoto, A. *Macromolecules* **1991**, *24*, 4904.
(21) Swislow, G.; Sun, S. T.; Nishio, I.; Tanaka, T. *Phys. Rev. Lett.* **1980**, *44*, 796.
(22) Sun, S. T.; Nishio, I.; Swislow, G.; Tanaka, T. *J. Chem. Phys.* **1980**, *73*, 5971.
(23) Huglin, M. B.; O'Donohue, S. J.; Radwan, M. A. *Eur. Polym. J.* **1989**, *25*, 543.
(24) Nakata, M. *Polymer* **1997**, *38*, 9.
(25) Miyaki, Y.; Einaga, Y.; Fujita, H. *Macromolecules* **1978**, *11*, 1180.
(26) Schulz, G. V.; Altgelt, K. *Makromol. Chem.* **1960**, *36*, 209.
(27) Chu, B.; Ying, Q.; Grosberg, A. Y. *Macromolecules* **1995**, *28*, 180.
(28) Yamakawa, H. *Macromolecules* **1993**, *26*, 5061.

MA049208L